DOI: 10.1002/chem.200600077

A Simple Hydrothermal Method for the Large-Scale Synthesis of Single-Crystal Potassium Tungsten Bronze Nanowires

Zhanjun Gu,[a, b] Ying Ma,[a] Tianyou Zhai,[a] Bifen Gao,[a] Wensheng Yang,[c] and Jiannian Yao*[a]

Abstract: The large-scale synthesis of single-crystal K_xWO_3 tungsten bronze nanowires has been successfully realized by a hydrothermal method under mild conditions. Uniform $K_{0.33}WO_3$ nanowires with diameters of 5–25 nm and lengths of up to several micrometers are obtained. It is found that the morphology and crystallographic forms of the final products are strongly dependent on the sulfate and citric acid, which may act as structure-directing and soft-reducing agent, respectively. Some other influential factors on the growth of tungsten bronze nanowires, such as temperature and reaction time, are also discussed. It is worth noting that other alkali metal tungsten bronzes such as $(NH_4)_xWO_3$, Rb_xWO_3, and Cs_xWO_3 could also be selectively synthesized by a similar route. Thus, this novel and efficient method could provide a potential mild route to selectively synthesize various tungsten bronze on-dimensional nanomaterials.

Keywords: crystal growth · hydrothermal synthesis · nanostructures · tungsten

Introduction

There has been recent heightened interest in one-dimensional nanoscale building blocks, such as nanotubes, nanowires, and nanorods because of their distinctive geometries, novel physical and chemical properties, and potential applications in nanodevices.[1,2] A number of methods have been developed for the preparation of 1D nanostructures, such as applying electrochemical techniques,[3] porous aluminum templates,[4] as well as vapor–liquid–solid (VLS) growth[5,6] and vapor–solid (VS) reactions.[7] Solution approaches have been shown to provide an alternative route for the synthesis of 1D nanostructures, with the advantages of mild synthetic conditions, simple manipulation, and large-scale production.[8] The hydrothermal method, in particular, has been successfully applied for the synthesis of various metal and semiconductor nanorods/nanowires/nanotubes.[9–12]

Tungsten bronzes have attracted much attention in the past few decades due to their wide variety of crystal structures and interesting electro-optic, photochromic, and superconducting properties.[13] Consequently, they have been applied in electronic devices, humidity and gas sensors, and secondary batteries.[14] In particular, the hexagonal alkali tungsten bronzes A_xWO_3 (HTBs, A = K, Rb, Cs, and NH_4; $0 < x < 1/3$) have been the subject of numerous studies.[15,16] The traditional methods for the preparation of the hexagonal tungsten bronze structure require high temperatures and harsh reaction conditions, such as heating mixtures of WO_3 with K, Rb, or Cs in reducing atmospheres at 1000 °C.[17] Recently, more attention has been paid to the low-temperature solution-based methods.[18] Whittingham et al. reported the hydrothermal synthesis of various novel tungstates with pyrochlore and hexagonal tungsten bronze structures that are not attainable by traditional high-temperature solid-state reactions.[19] Theses tungstates were completely oxidized compounds and tended to have the general formula $A_xWO_{3+x/2}$. Mathiram et al. reported a new sol–gel route to prepare sodium tungsten bronze by reduction of sodium tungsten with $NaBH_4$ in aqueous solution, followed by crystallization

[a] Dr. Z. J. Gu, Dr. Y. Ma, Dr. T. Y. Zhai, Dr. B. F. Gao, Prof. J. N. Yao
Key Laboratory of Photochemistry
Centre for Molecular Sciences
Institute of Chemistry
Chinese Academy of Sciences
Beijing (100080) (P.R. China)
Fax: (+86) 10-8261-6517
E-mail: jnyao@iccas.ac.cn

[b] Dr. Z. J. Gu
Graduate School of the Chinese Academy of Science
Beijing (100080) (P.R. China)

[c] Prof. W. S. Yang
College of Chemistry
Jilin University
Changchun, 130023 (P.R. China)

Supporting information for this article is available on the WWW under http://www.chemeurj.org/ or from the author.

at 700 °C.[20] However, most of the synthetic routes only led to bulk materials, and the synthesis of HTBs with a 1D nanostructure is still a challenge to material scientists. Since the 1D nanostructured HTBs may be anticipated to have unique properties, the synthesis of one-dimensional HTB nanostructures is of special interest and of great importance. To the best of our knowledge, a large-scale synthesis of K_xWO_3 nanowires has not been achieved up till now. Furthermore, there is no report on a simple solution method for the selective preparation of various HTB nanorods/nanowires. Recently we have obtained 1D nanostructures for the hexagonal phase of WO_3 by hydrothermal treatment of the WO_3 (sol) in the presence of Li_2SO_4.[21]Thus, it was anticipated that the various reduced 1D tungsten bronzes could be obtained by adding an appropriate mild reducing agent and various sulfates under similar hydrothermal conditions.

Herein, we report a convenient and controllable approach for the synthesis of K_xWO_3 single-crystal nanowires by adding citric acid and K_2SO_4. Our experiments have revealed that citric acid can act as both the acidification and reducing agent and its use has enabled us to prepare the pure phase of hexagonal K_xWO_3 nanowires on a large scale. This synthetic process is simple, mild, clean, low-cost, and template-free. Thus, this approach was deemed worthy of extending further for the convenient and large-scale synthesis of a family of molybdenum bronze or vanadium bronze 1D naonomaterials.

Results and Discussion

Characterization of the structure and morphology of K_xWO_3 nanowires: Hydrothermal treatment of the WO_3 (sol) precursor in the presence of citric acid and K_2SO_4 at 180 °C for 24 h led to the formation of single-crystal K_xWO_3 nanowires. Figure 1a shows a typical X-ray diffraction (XRD) pattern for the as-synthesized crystalline K_xWO_3 nanowires. All the reflections can be indexed to the hexagonal potassium tungsten bronze $K_{0.33}WO_3$ (JCPDS file No. 49-0541) and no impurities were identified in the XRD pattern. According to the reflections of the ground powder, the lattice constants are calculated to be 7.378 Å and 7.580 Å, which are similar with those reported in the literature [JCPDS file No. 49-0541]. In the XRD pattern of the nanowires, the intensity of the (002) reflection increases distinctly and that of the (100) reflection decreases visibly, suggesting the preferential growth of K_xWO_3 nanowires along the [001] direction. This supposition can be confirmed by from the HRTEM image. Like all tungsten bronzes, the hexagonal structure comprises a rigid tungsten–oxygen framework built up of layers containing corner-sharing WO_6 octahedron that are arranged in six-membered rings. The layers are stacked along [001] axis, leading to one-dimensional hexagonal channels, which are occupied randomly by potassium ions (Figure 1b).[22]

The chemical nature (i.e. oxidation state) of the tungsten and the potassium/tungsten ratio in the samples were determined by X-ray photoelectron spectroscopy (XPS). Figure 2

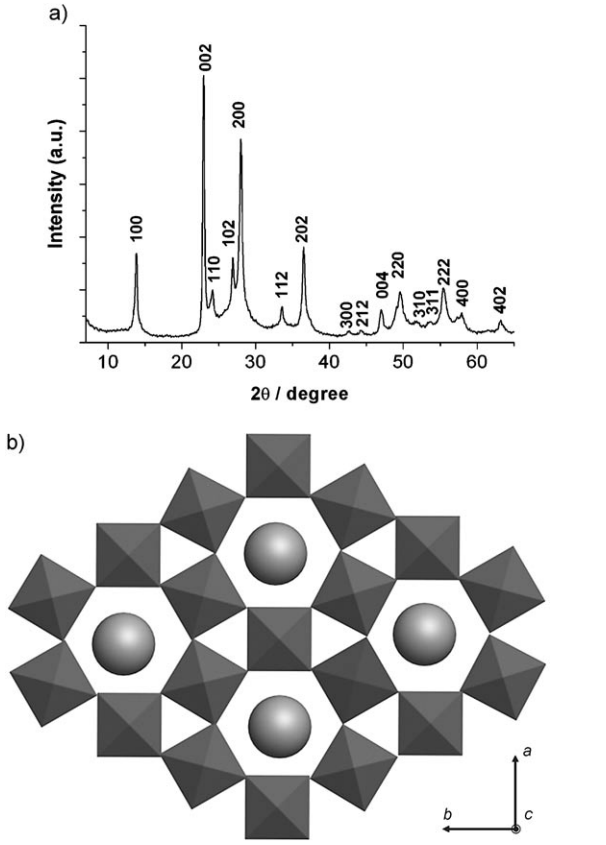

Figure 1. a) XRD pattern of the as-synthesized products. b) Arrangement of $[WO_6]$ octahedral in the structure of hexagonal $K_{0.33}WO_3$. Cross-section in the *ab* plane perpendicular to the *c* axis. Potassium ions occupy these hexagonal channels randomly.

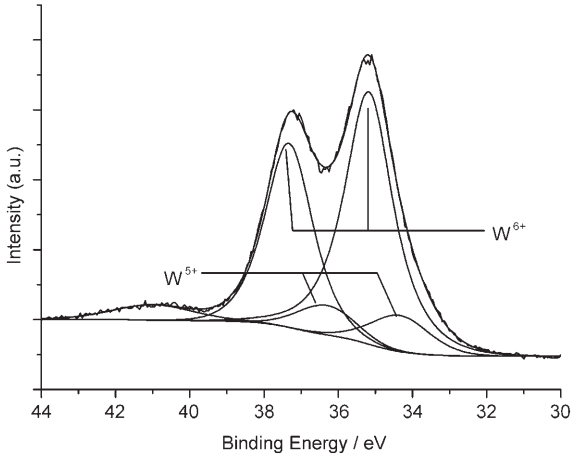

Figure 2. W4f core-level XPS spectrum of the $K_{0.33}WO_3$ nanowires.

shows the typical X-ray photoelectron spectrum of the tungsten core level (W4f) in the as-synthesized products. The curve can be fitted to two spin-orbit doublets, $W_{4f7/2}$ and $W_{4f5/2}$ for the distance of 2.1 eV. The peaks at 34.3, 36.4 eV and 35.3, 37.4 eV can be attributed to W^{5+} and W^{6+}, respec-

tively, which are in good agreement with the reported values (BE of 34.5 and 36.5 eV for W^{5+} and 35.8 and 37.9 eV for W^{6+}) in photochromic tungsten oxide thin films following exposure to UV light.[23] From the integrated areas of the potassium and tungsten (W4f) core level, we estimate that the ratio of K^+/WO_3 in the product was about 0.33 ± 0.03, which is in good agreement with XRD results.

Figure 3 presents typical scanning electron microscopy (SEM) images of the as-synthesized $K_{0.33}WO_3$ nanowires.

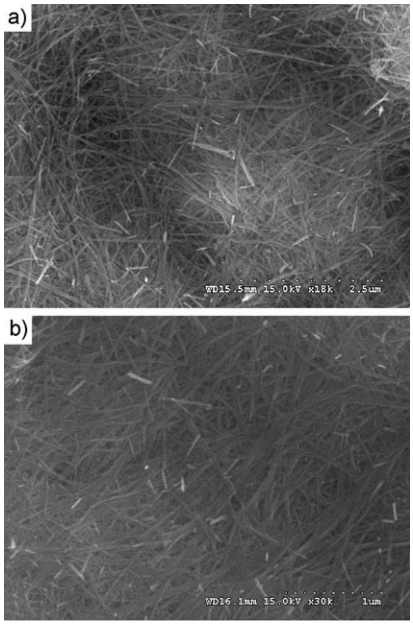

Figure 3. Representative SEM images of the $K_{0.33}WO_3$ nanowires. a) Overall morphology of the products. b) High-magnification SEM image of the nanowires.

The products exhibit exclusively 1D wirelike nanostructure with diameters typically in the range of 5–25 nm and lengths ranging from several hundred nanometers to several micrometers. Typical transmission electron microscopy (TEM) images of the $K_{0.33}WO_3$ nanowires (Figure 4) illustrate that these nanowires have a uniform diameter along their entire length. More details about the morphological and structural features were obtained from HRTEM measurements. The spacing of the lattice fringes are found to be about 0.639 and 0.379 Å, respectively (Figure 4b). These two planes can be well indexed as (100) and (001) planes of a hexagonal $K_{0.33}WO_3$ crystal, respectively, confirming that the nanowires are single crystals grown along the *c* axis. The energy-dispersive spectra (EDS) of the nanowires show that only K, W, and O are contained in the nanowires (Figure 4c).

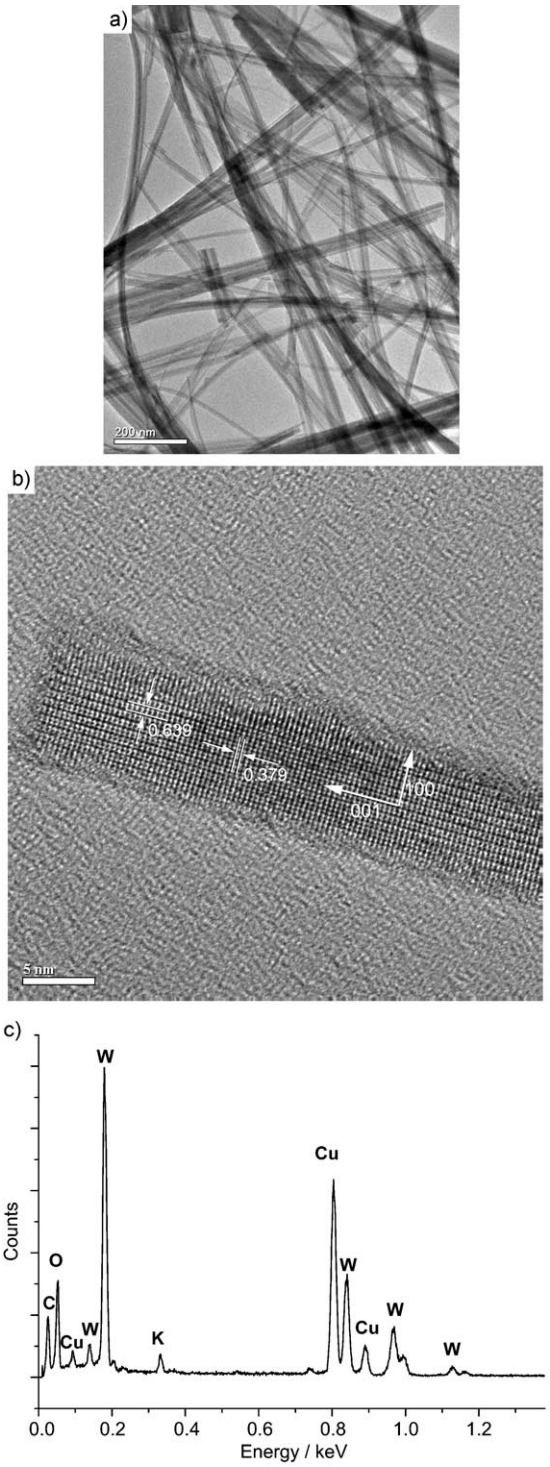

Figure 4. a) TEM image of the tungsten bronze nanowires. b) HRTEM image of a single $K_{0.33}WO_3$ nanowire with growth direction [001]. c) EDS data for the nanowires in which the Cu and C peaks were generated from the supporting carbon-coated copper meshes.

Influential factors and formation mechanism of the hexagonal potassium tungsten bronze 1D nanostructure: To investigate the growth process of the $K_{0.33}WO_3$ nanowires, we conducted experiments at 180 °C and varied the reaction times. An examination of the intermediate products showed that there were a large number of irregular particles after reaction for 1 h (Figure 5a). The intermediates collected after 2 h were even larger particles, but their surfaces were completely covered by small nanorods (Figure 5b). Over the

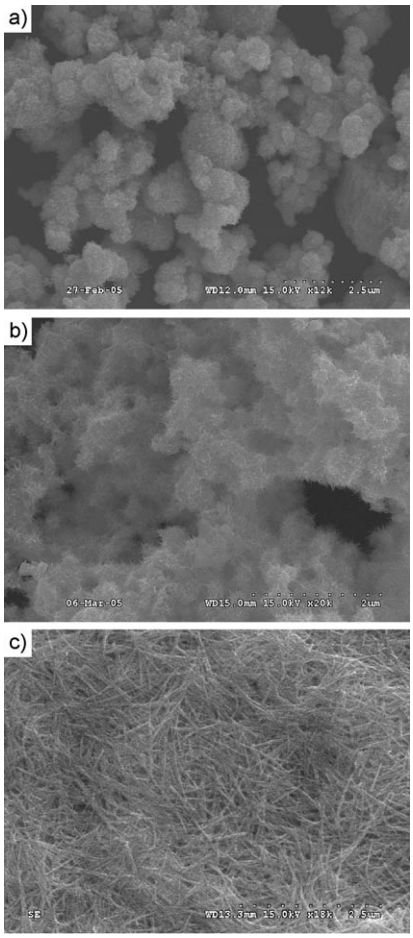

Figure 5. SEM images of intermediate products. After a) 1 h, b) 2 h, and c) 24 h.

course of the reaction, the irregular particles gradually vanished and longer nanorods appeared, suggesting that the longer nanorods grow at the cost of the irregular particles. After a reaction time of 24 h, single-crystalline hexagonal tungsten bronze nanowires with diameters of between 5 and 25 nm and lengths of between 0.5 and 2 μm were observed (Figure 5c). Although the length of the nanowires can be increased with prolonged reaction time, the diameter of the nanowires was shown to be only slightly dependent on the reaction time. In addition, the color of the products changes from yellow, through green to dark blue as the reaction proceeds, which suggests that reduction occurs with increasing reaction time. The reaction temperature also has a significant influence on the formation of nanowires. When the temperature was lower than 120 °C, no products were generated even when the reaction time was extended to 24 h. The optimum temperature for the rapid production of highly crystalline nanowires is as high as 180 °C.

It is apparent that the sulfate plays an important role in determining the crystal structure and morphology of the products. When the experiment was conducted in the absence of K_2SO_4, only irregular nanoparticles were obtained from the hydrothermal treatment at 180 °C for 24 h. When 0.3 g K_2SO_4 were used, a large number of short rods grew on the surface of the irregular particles. Results from the XRD characterizations show that the products were composed of the mixture of hexagonal WO_3 and $K_{0.33}WO_3$. (JCPDS card 33-1387 and JCPDS card 49-0541). This indicates that the incipient particles were not completely transformed into $K_{0.33}WO_3$ nanowires due to insufficient K_2SO_4. A pure hexagonal phase containing only $K_{0.33}WO_3$ nanowires was obtained by adding about 0.5 g K_2SO_4 (Figure 6). Two-dimensional assembly of these nanowires occurs spontaneously on a silicon wafer after evaporation of the solvent; these nanocrystals display a regular shape, high aspect ratio, and narrow size distribution (Figure 6c). To investigate the influence of different anions on the formation of HTB nanowires, other inorganic salts such as KCl, KBr, KNO_3, and $KHCO_3$ were also tested in this work. Our results show that these anions only led to the formation of irregular particles.

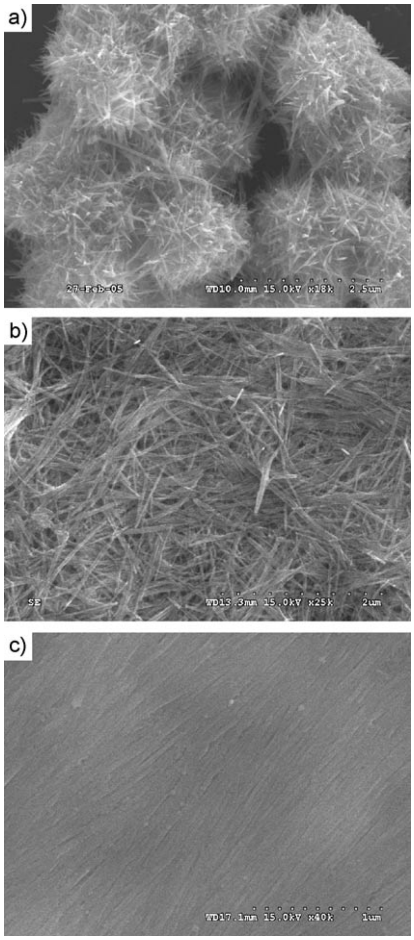

Figure 6. SEM images for our products prepared by adding 0.3 g (a) and 0.5 g K_2SO_4 (b). c) SEM image of the self-assembly of the nanowires on a silicon wafer after evaporation of the solvent.

Based on the above experimental results, a possible formation mechanism of the $K_{0.33}WO_3$ nanowires is proposed as follows:

1. In the synthetic process, SO_4^{2-} may act as a capping agent preferentially adsorbed on the faces parallel to the *c* axis of the $K_{0.33}WO_3$ nanocrystal, leading to preferential growth along the *c* axis.[24–26]
2. An appropriate mild reducing agent can be regarded as the key factor in the synthesis of $K_{0.33}WO_3$ nanowires. Our experiments have revealed that citric acid can function both as the acidification and reducing agent and has enabled us to prepare the $K_{0.33}WO_3$ nanowire on a large scale. Other reducing agents, such as $NaBH_4$, tartaric acid, and ascorbic acid were also used in this work but only irregular particles were obtained.
3. The studies of the intermediates reveal that there are two growing stages during the formation of the nanowires. At the beginning of the reaction, and with sufficient energy provided by the hydrothermal system, the nanoclusters are formed quickly and spontaneously aggregate to large particles to minimize their surface area. As the reaction proceeds, the concentration of the nanoclusters decreases sharply due to the formation of large particles. As a result, the crystal growth stage is a kinetically controlled process. Subsequent crystal growth is initiated preferentially from the active clusters on the surfaces of the particles, owing to the high concentration of SO_4^{2-} surrounding them. In the presence of sulfate, these clusters serve as seeds of the subsequent growth along the *c* axis of the K_xWO_3 unit cell, resulting in the formation of the nanorods. As the reaction proceeds the particles gradually vanish and longer nanowires appear, suggesting that the longer nanowires grow at the cost of the particles (Figure 7). This process was similar to the formation of Pt nanowires.[27] Other cases have also been encountered in the synthesis of MnO_2 and ZnO nanorod-based microspheres.[28,29]

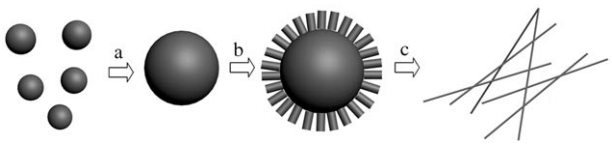

Figure 7. Proposed scheme for the formation of the nanowires. a) Formation of the particles. b) Growth stage of the nanowire. c) Formation of the $K_{0.33}WO_3$ nanowires with high aspect ratio.

UV/Vis absorption spectra and BET surface area: Figure 8 presents the UV/Vis reflectance diffuse spectrum of $K_{0.33}WO_3$ nanowires. These nanowires are blue in color. The reflectance measurements on the products show that the band gap absorption at the onset of the nanowires is around 450 nm, corresponding to the band gaps of WO_3 (2.8 eV). A broad absorption in the visible region can also be observed in the spectrum, which is attributed to the d–d transition of W^{5+} in WO_3. Analogous to the tungsten bronze of the H_xWO_3 type, the reduction leads to the insertion of electrons into the LUMO band of the overlapping d orbital,

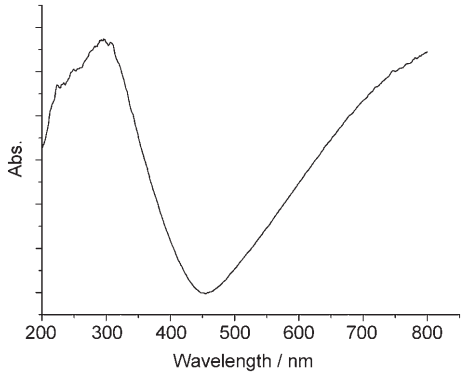

Figure 8. Diffuse reflectance UV/Vis spectra of the $K_{0.33}WO_3$ nanowires.

thus allowing d–d transitions to be observed in the visible region of the spectrum.[30] The N_2 Brunauer–Emmett–Teller (BET) surface area of the tungsten bronze nanowires is measured to be 59.0 $m^2 g^{-1}$, confirming the small size and high surface area of the products.

Synthesis of other alkali metal tungsten bronze 1D nanomaterials: Similarly, perfect single crystals of $(NH_4)_xWO_3$ nanorods could be selectively synthesized when $(NH_4)_2SO_4$ was used instead of K_2SO_4. The as-obtained products were characterized by X-ray powder diffraction (Figure 9a). The sample was readily indexed as hexagonal $(NH_4)_{0.33}WO_3$: $a=7.388$, $c=7.502$ Å, which is in good agreement with literature values (JCPDS Card No. 42-0452). Figure 9b shows the high-resolution XPS spectrum of our products in the W4f region. The peaks at 35.0 eV and 37.1 eV are ascribed to the $W4f_{7/2}$ and $W4f_{5/2}$ of W^{6+}. The binding energies at 34.1 eV and 36.2 eV correspond to the $W4f_{7/2}$ and $W4f_{5/2}$ of W^{5+}. The ratio of NH_4^+/WO_3 in the bronzes is about 0.33 as determined from the integrated areas of the N1s and W4f peaks. Figure 9c and 9d show typical SEM and TEM images of the as-synthesized $(NH_4)_{0.3}WO_3$ nanostructures. The products comprise pure wirelike nanostructures with diameters of 5–30 nm and lengths up to several hundred nanometers (Figure 9c). The TEM image (Figure 9d) suggests that the 1D nanostructure has a uniform diameter along its entire length.

Additional studies have shown that other alkali metal tungsten bronzes such as Rb_xWO_3 and Cs_xWO_3 can also be selectively synthesized by applying a similar method (see Supporting Information). Thus, the present approach could be a general approach for the synthesis of other tungsten bronze 1D nanostructures, such as rare-earth metal, alkali-earth metal, and transition-metal tungsten bronzes. In it anticipated that these low-dimensional materials will find important applications in various fields. Further detailed studies on these new kinds of 1D nanobuilding blocks are in progress.

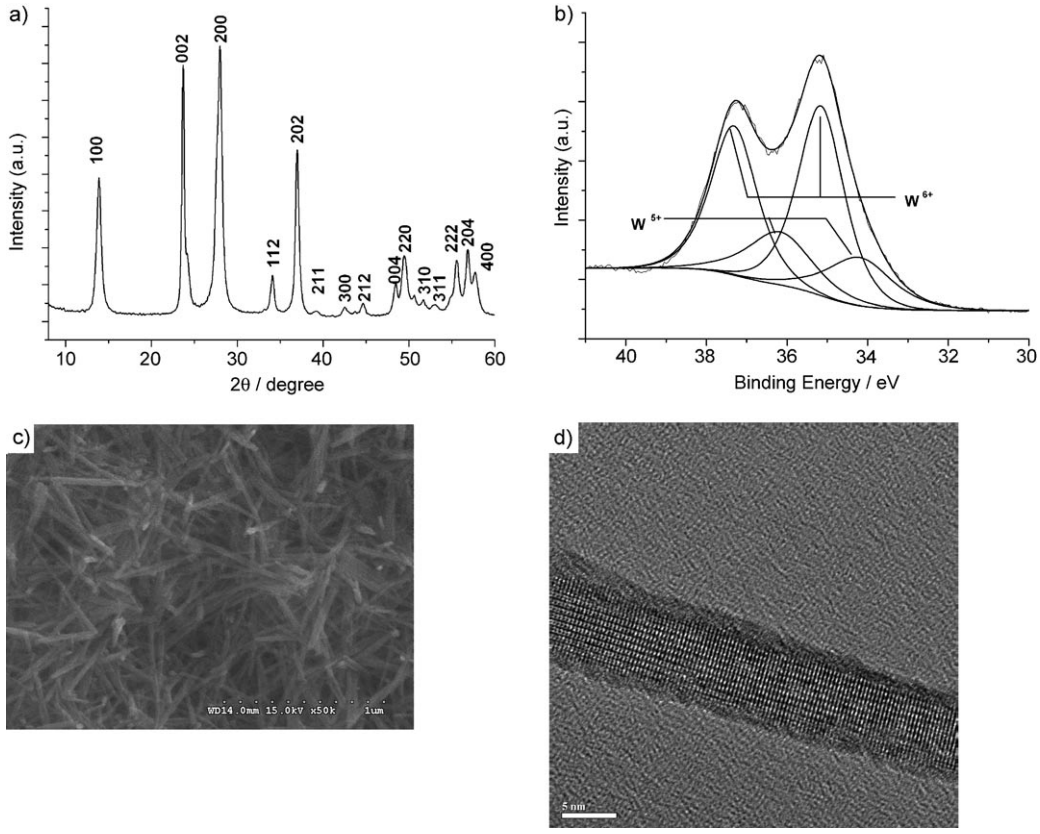

Figure 9. a) XRD pattern for the prepared $(NH_4)_{0.33}WO_3$ nanowires. b) W4f core-level XPS spectrum of the $(NH_4)_{0.33}WO_3$ nanowires. SEM (c) and TEM images (d) of $(NH_4)_{0.3}WO_3$ nanowires obtained after hydrothermal treatment at 180 °C for 24 h.

Conclusion

In conclusion, we have developed a simple hydrothermal reduction method to synthesize uniform hexagonal tungsten bronze (HTB) $K_{0.33}WO_3$ single-crystal nanowires on a large scale. The formation mechanism of the nanowires has been investigated. The citric acid and sulfate clearly contribute to the creation of the HTB 1D nanomaterials. This new strategy has beed applied to prepare other tungsten bronze 1D nanomaterials. A wider ranging application of this method is under investigation, since it is a simple, mild solution method with promising advantages over the traditional high-temperature approach for the rational design and large-scale production of one-dimensional tungsten bronzes. These low-dimensional tungsten bronze nanocrystals may open new opportunities for further investigation of the novel optical, electric, and catalytic properties of these materials.

Experimental Section

Materials: All the chemicals were of analytical grade and used without further purification. Potassium sulfate (K_2SO_4), ammonium sulfate ($(NH_4)_2SO_4$), citric acid monohydrate ($C_6H_8O_7{\cdot}H_2O$), potassium tungstate (K_2WO_4) were purchased from the Beijing Chemical Reagent Company.

Synthesis: In a typical experiment, the WO_3 sol was prepared in advance as follows: potassium tungstate powder (8.15 g, 0.025 mol) was dissolved in distilled water (250 mL). Then K_2WO_4 solution was acidified to a pH of 1–1.2 using HCl (3 mol L^{-1}) solution. The white precipitate was filtered, washed sequentially with water and ethanol to remove contaminant ions. Then, this precipitate was dispersed with citric acid (0.1 mol L^{-1}) solution to obtain a translucent, homogeneous and stable WO_3 sol. The WO_3 sol (15 mL) was transferred to a 20-mL autoclave, then a certain amount of K_2SO_4 was added, the autoclave was then sealed and maintained at 120–180 °C for 2–72 h. The dark blue products were filtered off, washed several times with distilled water and absolute ethanol, and finally dried in a vacuum at room temperature. Following the above procedures, pure hexagonal phase $K_{0.33}WO_3$ nanowires were obtained on a large scale. To study the formation process of the HTB nanowires, the experimental parameters were varied during the synthesis. The best yield obtained in our experiments was about 30%. Other tungsten bronze nanowires such as $(NH_4)_{0.33}WO_3$, Rb_xWO_3, and Cs_xWO_3 could be selectively synthesized by adding appropriate sulfates.

Characterization: XRD analysis was performed using a Japan Rigaku D/max-2500 diffractometer with $Cu_{K\alpha}$ radiation ($\lambda = 1.5418$ Å). The sizes and shapes of the nanowires were observed on a field-emission scanning electron microscope (SEM, Hitachi, S-4300) and a high-resolution transmission electron microscope (HRTEM, JOEL JEM-2010 operated at 200 kV). XPS measurements were carried out with an ESCALab220i-XL spectrometer by using a twin-anode $Al_{K\alpha}$ (1486.6 eV) X-ray source. All the spectra were calibrated to the binding energy of the adventitious C1s peak at 284.6 eV. The base pressure was about 3×10^{-7} Pa. For diffuse reflectance UV/Vis measurements, a Lambda 35 UV/Vis spectrometer (Perkin Elmer) was used in the diffuse reflectance mode. The spectral range measured was between 200 and 800 nm with a scan speed of 60 nm min^{-1} and a spectral resolution of 2 nm. Nitrogen adsorption of the

h-$K_{0.33}WO_3$ nanowires was measured at 77 K with an ASAP 2010 micrometritics degassed at 300 °C for several hours under vacuum.

Acknowledgements

This work was supported by the National Natural Science Foundation of China (Nos. 50221201, 90301010, 50502033), and the Chinese Academy of Sciences.

[1] a) Y. N. Xia, P. Y. Yang, Y. G. Sun, Y. Y. Wu, B. Mayer, B. Gates, Y. D. Yin, F. Kim, H. Yan, *Adv. Mater.* **2003**, *15*, 353–389; b) G. R. Patzke, F. Krumeich, R. Nesper, *Angew. Chem.* **2002**, *114*, 2554–2571; *Angew. Chem. Int. Ed.* **2002**, *41*, 2446–2461.
[2] a) X. Duan, Y. Huang, R. Agarwal, C. M. Lieber, *Nature* **2003**, *421*, 241–245; b) R. Q. Zhang, Y. Lifshitz, S. T. Lee, *Adv. Mater.* **2003**, *15*, 635–640; c) Z. W. Pan, Z. R. Dai, Z. L. Wang, *Science* **2001**, *291*, 1947–1949; d) Y. G. Sun, B. Gates, B. Mayers, Y. N. Xia, *Nano Lett.* **2002**, *2*, 165–168; e) Z. A. Peng, X. G. Peng, *J. Am. Chem. Soc.* **2002**, *124*, 3343–3353.
[3] Y. zhou, S. H. Yu, X. P. Cui, C. Y. Wang, Z. Y. Chen, *Chem. Mater.* **1999**, *11*, 545–546.
[4] a) X. Y. Zhang, L. D. Zhang, Y. Lei, L. X. Zhao, Y. Q. Mao, *J. Mater. Chem.* **2001**, *11*, 1732; b) Y. J. Han, J. M. Kim, G. D. Stucky, *Chem. Commun.* **1999**, 1683–1684.
[5] a) X. F. Duan, C. M. Lieber, *Adv. Mater.* **2000**, *12*, 298–302; b) C. J. Barrelet, Y. Wu, D. C. Bell, C. M. Lieber, *J. Am. Chem. Soc.* **2003**, *125*, 11498–11499.
[6] Z. W. Pan, Z. R. Dai, C. Ma, Z. L. Wang, *J. Am. Chem. Soc.* **2002**, *124*, 1817–1822.
[7] a) Z. R. Dai, Z. W. Pan, Z. L. Wang, *J. Am. Chem. Soc.* **2002**, *124*, 8673–8680; b) J. Y. Lao, J. Y. Huang, D. Z. Wang, Z. F. Ren, *Nano Lett.* **2003**, *3*, 235–238.
[8] a) Z. A. Peng, X. G. Peng, *J. Am. Chem. Soc.* **2001**, *123*, 1389–1395; b) Y. G. Sun, Y. N. Xia, *Adv. Mater.* **2002**, *14*, 833–837; c) X. G. Wen, W. X. Zhang, S. H. Yang, Z. R. Dai, Z. L. Wang, *Nano Lett.* **2002**, *2*, 1397–1401.
[9] a) X. J. Cui, S. H. Yu, L. L. Li, L. Biao, H. B. Li, M. S. Mo, X. M. Liu, *Chem. Eur. J.* **2004**, *10*, 218–223; b) S. H. Yu, L. Biao, M. S. Mo, J. H. Huang, X. M. Liu, Y. T. Qian, *Adv. Funct. Mater.* **2003**, *13*, 639–647; c) Z. H. Wang, J. W. Liu, X. Y. Chen, J. X. Wan, Y. T. Qian. *Chem. Eur. J.* **2005**, *11*, 160–163.
[10] G. T. Zhou, X. H. Wang, J. C. Yu, *Cryst. Growth Des.* **2005**, *5*, 1761–1765.
[11] X. W. Lou, H. C. Zeng, *Inorg. Chem.* **2003**, *42*, 6169–6171.
[12] J. F. Liu, Q. H. Li, T. H. Wang, D. P. Yu, Y. D. Li, *Angew. Chem.* **2004**, *116*, 3915–3919; *Angew. Chem. Int. Ed.* **2004**, *43*, 5048–5052.
[13] a) K. S. Lee, D. K. Seo, M. H. Whangbo, *J. Am. Chem. Soc.* **1997**, *119*, 4043–4049; b) S. Reich, Y. Tsabba, *Eur. Phys. J.* **1999**, *B9*, 1–4.
[14] a) J. V. Dobson, J. Coiner, *J. Electroanal. Chem.* **1987**, *220*, 225–234; b) M. A. Wechter, H. R. Shanks, G. Carter, G. M. Ebert, R. Guglielmio, A. F. Voigt, *Anal. Chem.* **1972**, *44*, 850–853.
[15] a) T. Kudo, A. Kishimoto, H. Inoue, *Solid State Ionics* **1990**, *40*/41, 567–571; b) H. B. Krause, W. G. Moulton, R. C. Morris, *Acta Crystallogr. Sect. B* **1985**, *41*, 11–21.
[16] L. H. Cadwell. R. C. Morris, W. G. Moulton, *Phys. Rev. B* **1981**, *23*, 2219–2223.
[17] a) S. V. Vakarin, A. N. Baraboshkin, K. A. Kaliev, V. G. Zyrianov, *J. Cryst. Growth* **1995**, *151*, 121–126; b) X. Miao, *J. Cryst. Growth* **1999**, *197*, 1008–1011.
[18] a) J. H. Zhan, X. G. Yang, Y. Xie, B. F. Li, Y. T. Qian, Y. B. Jia, *Solid State Ionics* **1999**, *126*, 373–377; b) R. Fan, X. H. Chen, Z. Gui, S. Y. Li, Z. Y. Chen, *Mater. Lett.* **2001**, *49*, 214–218.
[19] a) K. P. Reis, A. Ramanan, M. S. Whittingham, *J. Solid State Chem.* **1992**, *96*, 31–47; b) K. P. Reis, A. Ramanan, M. S. Whittingham, *Chem. Mater.* **1990**, *2*, 219–221; c) K. P. Reis, E. Prince, M. S. Whittingham, *Chem. Mater.* **1992**, *4*, 307–312.
[20] Y. T. Zhu, A. Mathiram, *J. Solid State Chem.* **1994**, *110*, 187–189.
[21] Z. J. Gu, Y. Ma, W. S. Yang, G. J. Zhang, J. N. Yao, *Chem. Commun.* **2005**, 3597–3599.
[22] C. S. Griffith, V. Luca, *Chem. Mater.* **2004**, *16*, 4992–4999.
[23] D. G. Barton, M. Shtein, R. D. Wilson, S. L. Soled, E. Iglesia, *J. Phys. Chem. B* **1999**, *103*, 630–640.
[24] a) X. Wang, Y. D. Li, *J. Am. Chem. Soc.* **2002**, *124*, 2880–2881; b) X. Wang, Y. D. Li, *Chem. Eur. J.* **2003**, *9*, 300–306.
[25] G. R. Patzke, A. Michailovski, F. Krumeich, R. Nesper, J. D. Grunwaldt, A. Baiker, *Chem. Mater.* **2004**, *16*, 1126–1134.
[26] A. Michailovski, F. Krumeich, G. R. Patzke, *Helv. Chim. Acta* **2004**, *87*, 1029–1047.
[27] J. Y. Chen, T. Herricks, M. Geissler, Y. N. Xia, *J. Am. Chem. Soc.* **2004**, *126*, 10854–10855.
[28] Z. Q. Li, Y. Ding, Y. J. Xiong, Y. Xie, *Cryst. Growth Des.* **2005**, *5*, 1953–1958.
[29] M. Mo, J. Yu, L. Z. Zhang, S. K. A. Li, *Adv. Mater.* **2005**, *17*, 756–760.
[30] a) Y. P. He, Z. Y. Wu, L. M. Fu, C. R. Li, Y. M. Miao, L. Cao, H. M. Fan, B. S. Zou, *Chem. Mater.* **2003**, *15*, 4039–4045; b) S. Kuba, M. Che, R. K. Grasselli, H. Knözinger, *J. Phys. Chem. B* **2003**, *107*, 3459–3463.

Received: January 18, 2006
Revised: March 26, 2006
Published online: July 3, 2006

